Local rigidity and physical trends in embedded Si nanocrystals

K. Kleovoulou and P. C. Kelires

Research Unit for Nanostructured Materials Systems, Department of Mechanical and Materials Science Engineering, Cyprus University of Technology, P.O. Box 50329, 3603 Limassol, Cyprus

(Received 27 September 2013; revised manuscript received 14 November 2013; published 11 December 2013)

We investigate the problem of local rigidity of Si nanocrystals embedded in amorphous silica. By analyzing the elastic (bulk) modulus field into atomic contributions, we show that it is highly inhomogeneous. It consists of a hard region in the interior of the nanocrystals, with moduli ∼105 GPa, compared to 98 GPa for bulk Si, and of "superhard" (∼120 GPa) and "supersoft" (∼80 GPa) regions in the outer parts. Overall, the nanocrystal bulk modulus is significantly enhanced compared to the bulk, and its variation with size accurately follows a power-law dependence on the average bond length. The bulk modulus of the oxide matrix and of the interface region is nearly constant with size, with values 60 and 70 GPa, respectively. The average optical (homopolar) gap is directly linked to the elastic and bond-length variations.

DOI: 10.1103/PhysRevB.88.245202 PACS number(s): 61.46.Hk, 62.20.de, 62.23.Pq

Silicon nanocrystals (Si-NCs) embedded in amorphous silica[1] (a-SiO_2) are a prototypical nanomaterial system that has attracted considerable attention for its light absorption and emission properties. Promising applications include light-emitting devices,[2] nonvolatile memory systems,[3] and third-generation solar cells.[4,5] The fundamental properties of this nanocomposite system depend strongly on the size of the nanoinclusions and the nature of the embedding medium.[6]

Probably, the least studied and understood property of this system is the mechanical response of the embedded NC to the pressure exerted by its environment, as the NC size varies. The elucidation of this property is crucial not only for the mechanical stability, but for the optoelectronic properties as well.[7,8] A number of issues arise. The most important is whether the mechanical response of the NC, exemplified let us say by its elastic (bulk) modulus, is uniform throughout the NC or varies substantially from region to region, or from the interior (core) to the interface with the matrix. Another issue is whether any variations in the modulus follow definite trends, and how these physical trends can be associated to other NC properties.

Previous theoretical studies[9,10] on free-standing or colloidal NCs predicted enhancement of the bulk modulus as the size decreases, which was attributed to either surface effects[9] or to the strong interaction of the NC with passivants such as H.[10] The enhancement is consistent with experimental measurements.[11] On the other hand, no theoretical study exists for embedded NCs, but experimental work on the compressibility of embedded Si-NCs/a-SiO_2 shows enhancement.[12] An analysis at the local level, able to separate the contributions to the modulus and rigidity from the NC core, the surface/interface, and the embedding matrix, is lacking.

Here, we elucidate these issues through atomistic Monte Carlo (MC) simulations. By utilizing a technique decomposing the elastic response of the system into atomic bulk moduli,[13] we unravel a striking effect. The rigidity of an embedded NC is not uniform, as it exhibits both "hard" and "soft" regions, arising from the structural inhomogeneity of the surrounding amorphous silica matrix and the oxygen bonding at the NC surface. Overall, the bulk modulus shows a significant enhancement from the bulk value, and the variation with size follows a well-defined physical trend. This is associated with a corresponding trend in the average optical gap of the material.

For our study, we use cubic computational cells consisting of spherical NCs embedded in a-SiO_2 matrices. They are obtained by continuous-space MC simulations,[14] using for the interactions the Tersoff empirical potential[15] parametrized to describe SiO_2 systems.[16] This potential describes well the elemental Si properties, silica polymorphs, and phase transitions between them, as well as the structure and energetics of a-SiO_2. We have recently shown the reliability and strength of this approach by extracting stress maps of embedded NCs,[6] intractable by *ab initio* calculations. We also verified that the calculated[6] bulk moduli of various polymorphs are in very good agreement with results of *ab initio* calculations[17] and experiment. This reassures us that the pressure exerted by the amorphous matrix on the nanocrystals is correct.

One starts with Si NCs embedded in crystalline β-cristobalite.[1] The amorphization of the embedding matrix is achieved by melting and subsequent quenching from the liquid, while keeping the positions of the atoms in the NCs fixed, running the simulations in the (N,V,T) canonical ensemble. After quenching, an annealing cycle at 1500 K in the (N,P,T) isobaric-isothermal ensemble follows to allow for full equilibration of the nanocomposite system, both geometrically and compositionally. This is crucial for the proper structural relaxation and the formation of optimum chemical bonding at the interface region that minimizes the free energy. Finally, the structures are brought to 300 K where all properties are obtained as ensemble averages.

We have generated in total seven different composite structures with the size of the NCs ranging from 1 to 5 nm in diameter, the number of Si atoms in the NC from 40 to 3600, and the number of atoms in the oxide from 4800 to 50 000. We keep the Si/O ratio at about 0.53 to consistently capture the variation of moduli with NC size. The cells are subjected to periodic boundary conditions so that the NCs properly interact with their images.

The key to our analysis of local rigidity is the concept of atomic bulk modulus, developed earlier by Kelires[13] for the study of amorphous carbon materials and other systems where the environment is more or less isotropic at the local

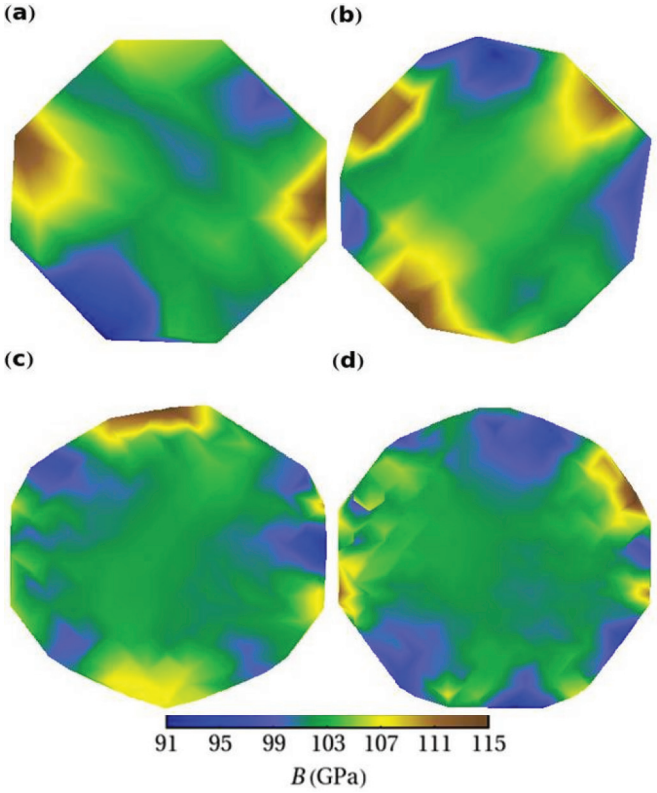

FIG. 1. (Color online) Contour maps of local bulk moduli in {110} planes (passing through the NC center), in the core of four representative NCs with sizes: (a) 2.2 nm, (b) 3 nm, (c) 4 nm, (d) 5 nm. The atomic moduli are merged into a continuous mesh by averaging over spheres of 3 Å in radius.

level. These conditions are fulfilled in each constituent of the nanocomposite system studied here. One starts with the decomposition of the total energy of the system E into atomic energies E_i, readily obtainable in the present empirical potential approach. The equilibrium atomic bulk modulus B_0^i, indicative of the local rigidity, is then defined as

$$B_0^i = \Omega_i \frac{d^2 E_i}{d\Omega_i^2}, \tag{1}$$

where Ω_i is the atomic volume (such as the Wigner-Seitz volume of atom i). The total bulk modulus B_0 is the normalized sum of the B_0^i over all atoms in the system, while normalized sums over atoms in specific regions can yield partial contributions, such as for the NC core, the interface, and the matrix. Equivalently, these partial contributions to the bulk modulus can be obtained through Murnaghan's equation of state[18] by summing up the atomic energies over the specified regions.

We begin with the local rigidity of the embedded NCs. (The microstruture of these nanocomposite systems has been described in detail previously.[6]) Figure 1 shows two-dimensional contour maps of atom-projected bulk moduli in the core region (composed of Si atoms having as neighbors only Si^{+0} suboxides, i.e., Si atoms not bonded to any O atoms) of four representative NCs of various sizes. There are two striking findings in these maps. The first is that in all cases the field of atomic moduli, and thus of local rigidity, is

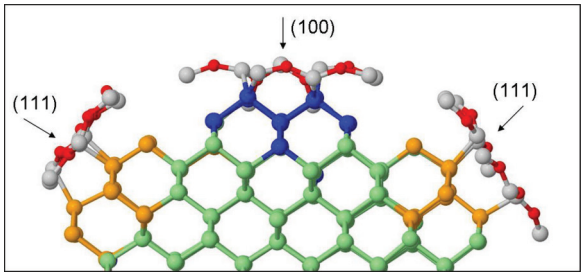

FIG. 2. (Color online) Ball and stick model (part of a thin slice cut) of a Si NC (3 nm) showing the bridge-bonding reconstructions of {111} and {100} facets and the local modulus field in the NC core beneath. The matrix and some atoms at the interface are not shown for clarity. Si and O atoms in the bridges are colored gray and red, respectively. Sites colored orange (blue) possess moduli over (under) 110 (90) GPa. Sites deeper in the core (green) have moduli around 105 GPa.

highly inhomogeneous, not only while moving from the center outwards but along the periphery as well. The other is that the NCs exhibit both hard (more rigid) regions, with moduli approaching 115 to 120 GPa, compared to the bulk value of 98 GPa, and soft (less rigid) regions with moduli around 85 to 90 GPa. These hard and soft regions are mainly found in the outer regions near the interface and roughly alternate each other. The center possesses overall hard regions but with somewhat lower moduli, around 105 GPa.

We may explain this surprising effect by noting that the density and microstructure of the surrounding silica matrix is not homogeneous. It exhibits substantial variations from region to region. As a result, the strain produced by the matrix on the outer regions of the NC varies from place to place, and this propagates into the interior giving rise to an inhomogeneous pattern. Another contributor to the effect is bridge (Si-O-Si) bonding at the NC surface, which induces significant strains in the layers below. These strains differ depending on the crystallographic orientation of the NC. For example, bridges in the Si(111) planar interface produce compression underneath, while bridges in the Si(100) interface produce tension.[19] A Si NC encompasses all crystallographic orientations, and thus both compressed and tensed outer regions appear.

These induced strains are associated with the degree of local rigidity. This is illustrated in Fig. 2, showing that the core regions just under the {111} facets of a representative NC are "superhard" with moduli over 110 GPa, while regions under the {100} facets are "supersoft" with moduli less than 90 GPa. The former regions contain on average sites under compression with shorter bonds, compared to the bulk, while the latter contain sites under tension with longer bonds. This bridge-bonding effect produces the hard/soft alternating outer patterns evidenced in Fig. 1, which are however blurred by the inhomogeneous matrix effect. The latter effect becomes overwhelming when the whole spherical NC is visualized, that is taking into account all possible plane orientations which may or may not involve bridge bonding at the interface. The inner core region is overall "harder" than the bulk.

The direct link of local rigidity to bond-length variations is demonstrated in Fig. 3. Here, the atomic bulk moduli B_0^i are plotted as a function of the average length of the bonds that the

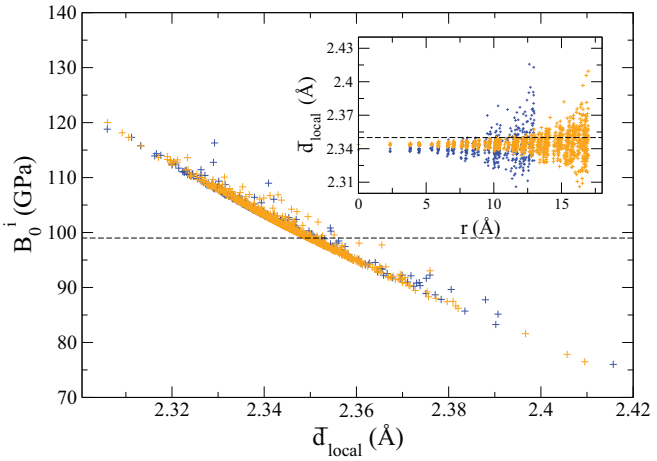

FIG. 3. (Color online) Atomic bulk moduli vs average bond length (see text). Orange (blue) symbols refer to NCs 3 (4) nm in size. Dashed horizontal line shows the bulk value. The inset shows how the average bond length varies from the center to the outer core regions.

reference atom makes with its first nearest neighbors (NN). The variation is linear and extends from "supersoft" sites with moduli as low as 75 GPa, involving largely stretched bonds compared to the bulk value, up to "superhard" sites with moduli as high as 120 GPa, involving heavily compressed bonds. The spatial distribution of bond lengths in the core of the NCs is seen in the inset of Fig. 3. Clearly, all bonds are compressed in the inner regions, which is consistent with the compressive stress behavior studied elsewhere,[6] and the related moduli are in the range of 105 GPa. As we move outwards, the distribution broadens considerably, and contains near the interface both compressed and stretched bonds, giving rise to the extrema in the moduli and the inhomogeneous patterns seen in Fig. 1.

Overall, the modulus of the core is significantly increased with respect to the bulk crystalline value. Its variation with size is shown in Fig. 4. It rises up sharply for small sizes and seems to retrieve slowly the bulk value for only much

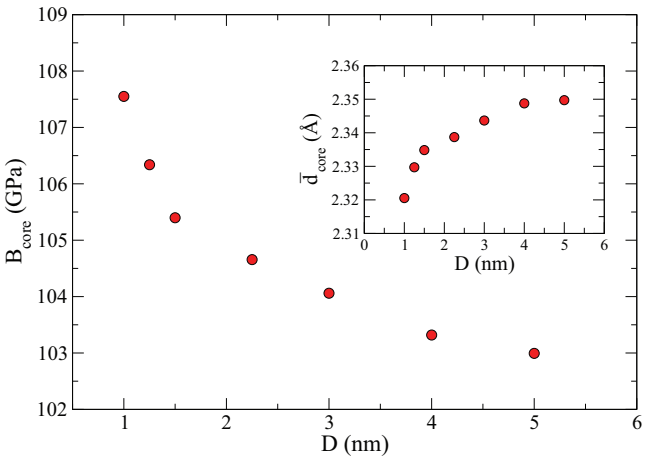

FIG. 4. (Color online) The average core bulk modulus as a function of the NC size. The inset shows how the average bond length in the NC core varies with size.

larger sizes than studied here. As shown in the inset of Fig. 4, the average bond length in the core drops with decreasing size, due to the increasing pressure exerted by the amorphous matrix because of the density mismatch.[6] As a result, this enhances the average modulus. Thus, here, in the embedding case, the mechanism leading to enhanced rigidity is different than in the free-standing or colloidal case where it was attributed to either surface effects[9] or to interactions with passivants.[10] In our case, interface effects are responsible for the inhomogeneity of the elastic modulus field, as explained above.

The decomposition into interface and matrix contributions, on the other hand, shows that their average modulus does not vary significantly with NC size. It remains nearly constant attaining values of 70 and 60 GPa, respectively. The much larger embedding medium is hardly affected by the small variations in NC size. Also, the interface width and the suboxide ratios remain practically constant with varying size.[1,6]

The variation of the average NC modulus with size, and effectively with the average bond length, can be linked to a very interesting physical trend. This trend is related to a model proposed in 1985 by Cohen[20] for the bulk moduli of diamond and zinc-blende crystalline solids. It defines a power-law dependence of B_0 on the first NN separation (bond length) d, in the form

$$B_0 = Ad^{-3.5}, \tag{2}$$

A being a numerical constant. The physical considerations behind this model are that B_0 depends predominantly on the covalent character of the bond, exemplified by a *homopolar gap* E_h, and only weakly on ionicity, and that E_h scales logarithmically as $d^{-2.5}$ against lattice constants between different rows of the periodic table, as suggested by Phillips.[21] This power-law behavior, with the same scaling exponent, was generalized by Kelires to hold for the whole composition range of complex semiconductor alloys,[22] and even for amorphous carbon materials.[23]

Applying this theory to the present embedded NC case confirms that the shorter the average bond length $\bar{d}$ in the NC, the larger its modulus. The dependence of B_0 on $\bar{d}$ is shown in Fig. 5 in a log-log plot. The data, although lying in a narrow range, closely follow a straight line, which indicates that $B_0 = A\bar{d}^n$. A line fit through the points gives for the slope n and the constant factor A the values –3.5 and 1970, respectively, when B_0 is measured in GPa and $\bar{d}$ in Å, in perfect agreement with theory. This provides a solid verification of the physical considerations behind this theory, and shows that the elastic and structural data from our equilibrated cells are accurately calculated.

The power-law dependence of B_0 on $\bar{d}$ implies also a definite trend in the variation of the homopolar gap E_h in Si NCs. E_h plays the role of an average optical gap (the average bonding-antibonding splitting). Although not the true optical gap, E_h still indicates how the optical properties can be simply linked to and depend on changes in the structural parameters. According to the approach developed by Kelires,[22,23] the variation of E_h with size can be given by

$$E_h(D) = E_h(\mathrm{Si})\left[\frac{B_0(D)}{B_0(\mathrm{Si})} \times \frac{\bar{d}(D)}{\bar{d}(\mathrm{Si})}\right], \tag{3}$$

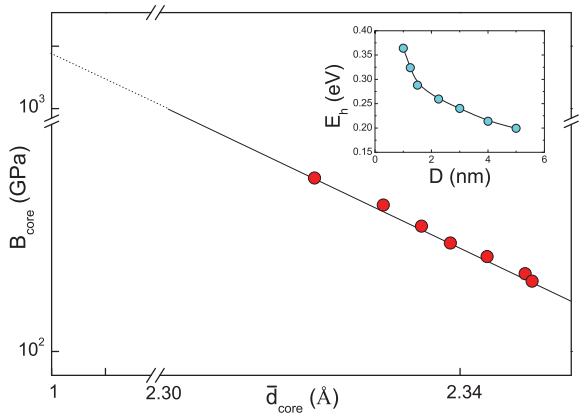

FIG. 5. (Color online) The NC bulk modulus as a function of the average NN distance. The range of data is magnified for clarity. The dashed line extrapolates to the constant A. The inset shows the variation of the homopolar gap with NC size relative to that of bulk Si (=5.07 eV).

where $E_h(D)$ is the size-dependent homopolar gap, and E_h(Si) and B_0(Si) are the homopolar gap (=5.07 eV) (Ref. 20) and bulk modulus of Si, used as the levels of reference. This approach is based on the argument[20] that for group-IV elements, the purest covalent materials with no ionic bonding, B_0 scales proportional to E_h, which measures the covalent character of the bond, and inversely proportional to the bond length d, $B_0 = FE_h d^{-1}$ (F is a numerical constant).

The results of this approach for $E_h(D)$ when applied to our case, given relative to E_h(Si), are plotted in the inset of Fig. 5. The overall variation retrieves precisely the $d^{-2.5}$ behavior, showing the reliability of our calculated moduli and bond lengths. $E_h(D)$ increases with decreasing size, especially for NCs smaller than 3 nm. Although $E_h(D)$ is not the true optical gap, its variation resembles the respective variations of the energy gaps and photoluminescence or absorption energies in this system as the NC size varies.[2,24] Even the magnitude of the enhancement falls within the experimental range. Thus, simple arguments, solely based on elastic and structural data, can give insight and useful trends without the need for elaborate electronic-structure calculations.

In relation to the above-mentioned optical properties, we may suggest that the major contributor of quantum confinement effects in the system is the observed shrinkage of the core of the NC, and the induced shortening of the bonds in this region. It is also very interesting to suggest that the large strains in the outer shell might decisively contribute to the strong absorption/emission centers in the NC. This issue has not yet been resolved. Work towards this goal is in progress.

In conclusion, our MC simulations and the accompanying local level analysis have been able to map in detail the elastic modulus field in Si-NC/a-SiO_2 nanocomposites and to unravel its origins. The field is found to be highly nonuniform in the NCs, exhibiting both hard and soft regions. Overall, the modulus is enhanced with respect to the bulk value, and follows a power-law behavior quite accurately. Variations in the optical parameters, such as the homopolar gap, can be linked to structural and elastic parameters in a simple way.

This work is supported by the Strategic Infrastructure Project NEW INFRASTRUCTURE/ΣΤΡΑΤΗ/0308/04 of DESMI 2008, which is cofinanced by the European Regional Development Fund, the European Social Fund, the Cohesion Fund, and the Research Promotion Foundation of the Republic of Cyprus.

[1] G. Hadjisavvas and P. C. Kelires, Phys. Rev. Lett. **93**, 226104 (2004); Physica E (Amsterdam) **38**, 99 (2007).
[2] L. Pavesi, L. Dal Negro, C. Mazzoleni, G. Franzo, and F. Priolo, Nature (London) **408**, 440 (2000).
[3] S. Tiwari, F. Rana, H. Hana, A. Hartstein, E. Crabbe, and K. Chan, Appl. Phys. Lett. **68**, 1377 (1996).
[4] G. Conibeer, M. Green, R. Gorkish, Y. Cho, E. Cho, C. Jiang, T. Fangsuwannarak, E. Pink, H. Huang, T. Puzzer, T. Trupke, B. Richards, A. Shalav, and K. Lin, Thin Solid Films **511**, 654 (2006).
[5] P. Löper, R. Müller, D. Hiller, T. Barthel, E. Malguth, S. Janz, J. C. Goldschmidt, M. Hermle, and M. Zacharias, Phys. Rev. B **84**, 195317 (2011).
[6] K. Kleovoulou and P. C. Kelires, Phys. Rev. B **88**, 085424 (2013).
[7] K. Kusová, L. Ondič, E. Klimešová, K. Herynková, I. Pelant, S. Daniš, J. Valenta, M. Gallart, M. Ziegler, B. Hönerlage, and P. Gilliot, Appl. Phys. Lett. **101**, 143101 (2012).
[8] R. Guerra and S. Ossicini, Phys. Rev. B **87**, 165441 (2013).
[9] G. Ouyang, X. L. Li, X. Tan, and G. W. Yang, Appl. Phys. Lett. **89**, 031904 (2006).
[10] R. Cherian, C. Gerard, P. Mahadevan, N. T. Cuong, and R. Maezono, Phys. Rev. B **82**, 235321 (2010).
[11] B. Gilbert, F. Huang, H. Zhang, G. Waychunas, F. Jilian, and F. Banfield, Science **305**, 651 (2004).
[12] S. H. Tolbert, A. B. Herhold, L. E. Brus, and A. P. Alivisatos, Phys. Rev. Lett. **76**, 4384 (1996).
[13] P. C. Kelires, Phys. Rev. B **62**, 15686 (2000).
[14] P. C. Kelires, Europhys. Lett. **14**, 43 (1991); Appl. Surf. Sci. **102**, 12 (1996); Int. J. Mod. Phys. **9**, 357 (1998); P. Sonnet and P. C. Kelires, Appl. Phys. Lett. **85**, 203 (2004).
[15] J. Tersoff, Phys. Rev. B **39**, 5566 (1989).
[16] S. Munetoh, T. Motooka, K. Moriguchi, and A. Shintani, Comput. Mater. Sci. **39**, 334 (2007).
[17] T. Demuth, Y. Jeanvoine, J. Hafner, and J. G. Angyan, J. Phys.: Condens. Matter **11**, 3833 (1999).
[18] F. D. Murnaghan, Proc. Natl. Acad. Sci. USA **30**, 244 (1994).
[19] D. Sander and H. Ibach, Phys. Rev. B **43**, 4263 (1991).
[20] M. L. Cohen, Phys. Rev. B **32**, 7988 (1985).
[21] J. C. Phillips, *Bonds and Bands in Semiconductors* (Academic, New York, 1973).
[22] P. C. Kelires, Phys. Rev. B **55**, 8784 (1997).
[23] C. Mathioudakis, G. Kopidakis, P. C. Kelires, C. Z. Wang, and K. M. Ho, Phys. Rev. B **70**, 125202 (2004).
[24] M. V. Wolkin, J. Jorne, P. M. Fauchet, G. Allan, and C. Delerue, Phys. Rev. Lett. **82**, 197 (1999).